

Global Hypoxia-Ischemia Induced Inflammation and Structural Changes in the Preterm Ovine Gut Which Were Not Ameliorated by Mesenchymal Stem Cell Treatment

Maria Nikiforou,^{1,2} Carolin Willburger,¹ Anja E de Jong,¹ Nico Kloosterboer,¹ Reint K Jellema,^{1,2} Daan RMG Ophelders,^{1,2} Harry WM Steinbusch,² Boris W Kramer,^{1,2,3} and Tim GAM Wolfs^{1,3}

¹Department of Pediatrics, Maastricht University Medical Center, Maastricht, The Netherlands; ²School for Mental Health and Neuroscience and ³School of Oncology and Developmental Biology, Maastricht University, Maastricht, The Netherlands

Perinatal asphyxia, a condition of impaired gas exchange during birth, leads to fetal hypoxia-ischemia (HI) and is associated with postnatal adverse outcomes including intestinal dysmotility and necrotizing enterocolitis. Evidence from adult animal models of transient, locally induced intestinal HI has shown that inflammation is essential in HI-induced injury of the gut. Importantly, mesenchymal stem cell (MSC) treatment prevented this HI-induced intestinal damage. We therefore assessed whether fetal global HI induced inflammation, injury and developmental changes in the gut and whether intravenous MSC administration ameliorated these HI-induced adverse intestinal effects. In a preclinical ovine model, fetuses were subjected to umbilical cord occlusion (UCO), with or without MSC treatment, and euthanized 7 d after UCO. Global HI increased the number of myeloperoxidase-positive cells in the mucosa, upregulated messenger RNA (mRNA) levels of interleukin (*IL*)-1 β and *IL*-17 in gut tissue and caused T-cell invasion in the intestinal muscle layer. Intestinal inflammation following global HI was associated with increased Ki67⁺ cells in the muscularis and subsequent muscle hyperplasia. Global HI caused distortion of glial fibrillary acidic protein immunoreactivity in the enteric glial cells and increased synaptophysin and serotonin expression in the myenteric ganglia. Intravenous MSC treatment did not ameliorate these HI-induced adverse intestinal events. Global HI resulted in intestinal inflammation and enteric nervous system abnormalities, which are clinically associated with postnatal complications, including feeding intolerance, altered gastrointestinal transit and necrotizing enterocolitis. The intestinal histopathological changes were not prevented by intravenous MSC treatment directly after HI, indicating that alternative treatment regimens for cell-based therapies should be explored.

Online address: <http://www.molmed.org>

doi: 10.2119/molmed.2015.00252

INTRODUCTION

Perinatal asphyxia is defined as a condition of impaired gas exchange during birth that leads to fetal hypoxia-ischemia (HI) and metabolic acidosis (1,2). Perinatal asphyxia is one of the most frequent causes of perinatal morbidity, accounting for approximately 23% of neonatal deaths worldwide (3,4). Fetuses that suffer from HI are at high

risk of developing multiorgan dysfunction (5,6), including the gut. HI-induced gut injury may result in adverse clinical outcomes, such as feeding intolerance, altered intestinal motility (7) and necrotizing enterocolitis (NEC), the most serious life-threatening gastrointestinal disease in neonates (8,9).

Numerous studies have recently demonstrated that the inflammatory

processes that follow intestinal HI play a key role in the pathophysiology of HI-induced gut injury (10–12). This evidence is primarily based on experiments in adult rodent models of transient superior mesenteric artery occlusion, showing that intestinal HI induces gut inflammation with concomitant epithelial lining loss, gut barrier dysfunction and morphological and functional changes in the muscle layers and enteric nervous system (ENS) (12–19). Although these studies provide insights into the mechanisms of HI-induced adverse intestinal outcomes, they represent the clinical scenario of locally induced intestinal HI in adults, whereas global HI, which occurs during perinatal asphyxia, leads to HI in multiple organs.

Systemic administration of mesenchymal stem cells (MSCs) has been tested as an

Address correspondence to Tim GAM Wolfs, Department of Pediatrics, Maastricht University Medical Center, Universiteitssingel 50, 6200 MD, The Netherlands. Phone: + 31-43-388-2232; Fax: + 31-43-387-5246; E-mail: tim.wolfs@maastrichtuniversity.nl.

Submitted December 8, 2015; Accepted for publication April 11, 2016; Published Online (www.molmed.org) April 14, 2016.

innovative therapeutic approach to modulate inflammation in a plethora of immune-mediated diseases (20). In particular, intravenous infusion of MSCs was proven to be successful in protecting the gut against inflammatory bowel diseases (21,22) and experimental NEC (23), two gastrointestinal pathologies that share some features with HI-induced injury of the adult intestine. We recently assessed the therapeutic potential of intravenous MSC administration in a preclinical model of global HI in the preterm ovine fetus, in which fetal global HI induced a systemic inflammatory response that was associated with structural and functional impairment of the fetal brain (24). These adverse effects of global HI on the fetal brain were substantially prevented by intravenous administration of MSCs, which are known to possess immunomodulatory, regenerative and reparative properties (25–27).

The aim of this study was therefore two-fold. First, to assess whether fetal global HI results in inflammatory and/or structural changes in the intestine. For this purpose, preterm fetal sheep were exposed to 25 min of transient umbilical cord occlusion (UCO) *in utero*. Second, we investigated whether intravenous administration of MSCs in this ovine model would ameliorate the global HI-induced adverse effects of the fetal intestine. To test our hypothesis, a clinically relevant intravenous dose of MSCs (28–30) was administered 1 h after UCO. We assessed the fetal ovine gut 7 d after UCO with respect to mucosal inflammation and injury, muscle abnormalities and changes in the ENS, as these pathophysiological characteristics contribute to feeding intolerance, altered gastrointestinal transit and NEC (31).

MATERIALS AND METHODS

Animals

All experiments were approved by the animal ethics committee of Maastricht University, the Netherlands, according to Dutch governmental regulations.

Experimental Procedures

Fetuses of time-mated Texel ewes were instrumented at 101 ± 0.9 d (mean \pm standard deviation [SD]) of gestation as previously described (24). Each ewe was anesthetized, and a catheter was placed in the maternal saphenous vein for pre- and postoperative administration of antibiotics and blood sampling. Each fetus was exposed by a midline incision, and catheters were placed in the femoral artery and brachial vein. In addition, electrodes were placed for electroencephalography (EEG) and electrocardiography (ECG) recordings, and an inflatable vascular occluder was placed around the umbilical cord to induce a hypoxic-ischemic insult. Finally, a catheter was placed in the amniotic cavity for amniotic fluid pressure measurements. The EEG, ECG and amniotic fluid pressure measurements have been previously reported by Jellema *et al.* (32). Each fetal catheter was exteriorized through a trocar hole in the flank of the ewe.

HI and MSC Administration

The experimental design of the study is depicted in Figure 1. The fetal sheep was used as a validated animal model to study the effects of fetal HI on organ development (33). In addition, fetal instrumentation *in utero* enabled us to test potential therapeutics to prevent organ damage after global HI (34–36). Fetal instrumentation was followed by a recovery period of 4 d as previously described (24). On day 105 ± 0.9 (mean \pm SD) of gestation (term approximately 147 d), fetuses were randomly assigned to an experimental group. The fetuses assigned to the HI group underwent 25 min of UCO to induce global HI, whereas the fetuses in the sham-UCO group were not occluded. Occlusion of the umbilical cord was confirmed by heart rate and arterial blood pressure recordings in conjunction with fetal blood gas analysis, demonstrating bradycardia, hypotension, acidemia, hypoxia and hypercapnia as previously reported (24). To induce an acute, sublethal asphyctic insult at this gestational age (GA) (0.7 of gestation), a 25-min

UCO was applied as previously reported (37). In addition, transient clamping of the umbilical cord for 25 min at this GA has been previously reported to result in fetal HI and cerebral and gastrointestinal hypoperfusion in ovine fetuses (37–40). One hour after the end of UCO (HI group, $n = 6$) or sham-UCO (control group, $n = 8$), saline or MSCs (HI + MSC group, $n = 7$) were given intravenously to the fetuses. The sham-UCO group received either saline (control group) or MSCs (MSC group, $n = 7$). MSCs were prepared at a dose of 3.5×10^6 MSCs (approximately 2.0×10^6 /kg) based on clinical trials of focal ischemia (28) and patients with inflammatory bowel disease (29,30). MSCs were given intravenously and were not associated with any signs of immunological rejection as previously described (32). At 113 d of gestation (7 d after the induction of UCO), both the ewes and fetuses were euthanized by pentobarbital (200 mg/kg). The rationale to euthanize the animals 7 d after UCO was based on the current feeding guidelines in the clinic, which indicate that enteral feeding is initiated approximately 7 d after birth and is gradually advanced in asphyxiated newborns. Therefore, to explore the underlying histopathological changes of the fetal gut after global HI, which might explain the clinical experience where the asphyxiated babies are not able to tolerate full enteral feeds at approximately 1 wk of age, we chose to euthanize our animals at exactly the moment that the enteral feeding would gradually start in the clinic. The survival rate in this model was 90%, and deceased animals were not included in the analyses. Importantly, autopsy of the dead animals revealed that fetal death was caused by technical reasons (e.g., arterial catheter not *in situ* resulting in exsanguination and subsequent fetal death, occluder obstructing the umbilical cord without inflation) and was unrelated to MSC treatment.

In this study, the GA of the fetal sheep is equivalent to a human premature baby of approximately 28–32 wks of gestation (37–41). Terminal ileum was examined,

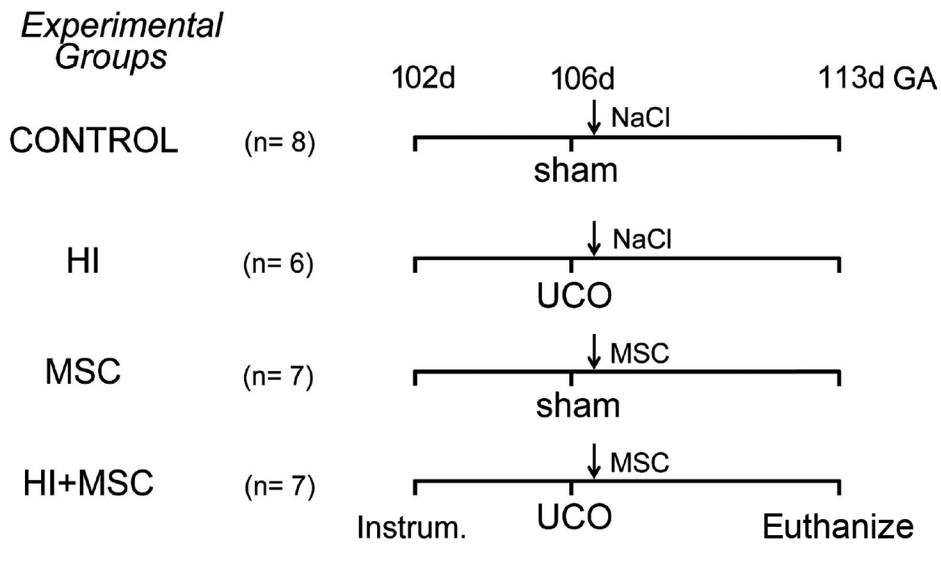


Figure 1. Experimental design of the study. Fetuses were instrumented at gestational age (GA) of 102 d. Four days after instrumentation (106 GA), umbilical cord occlusion (UCO) or sham was performed for 25 min followed by intravenous administration of either mesenchymal stem cells (MSCs) or saline (0.9% NaCl) 1 h after the end of UCO. The fetuses were euthanized 7 d after UCO or sham at 113 d of gestation.

as this region of the intestine is primarily affected in cases of perinatal asphyxia and NEC (42,43).

Preparation of Mesenchymal Stem Cells

Human bone marrow–derived MSCs (Merck Millipore) were isolated and prepared as previously described (32). Briefly, MSCs were isolated from a male donor, expanded, frozen and stored in liquid nitrogen. The MSCs were characterized by identifying cell surface molecules by flow cytometry analysis as previously described (32). MSCs were suspended in phosphate-buffered saline (PBS) 1 h before administration.

Antibodies

The following antibodies were used in this study: rabbit antibody against human CD3 and MPO (DAKO) for identification of T cells and neutrophils; mouse anti-SMA22 (gift of Dr. Olde Damink, Department of Surgery, Maastricht University, the Netherlands) for characterization of smooth muscle actin (SMA) present in circular and

longitudinal muscle layers; mouse anti-human Ki67 (DAKO) for detection of proliferating cells; mouse anti-synaptophysin (Millipore) for detection of presynaptic vesicle; monoclonal mouse anti-NeuN (Millipore) for detection of postmitotic neurons; polyclonal rabbit anti-5-hydroxytryptamine (anti-5-HT) custom-made in the Department of Neuroscience, Maastricht University, for identification of serotonin-expressing cells and polyclonal rabbit anti-glial fibrillary acid protein (GFAP) (DAKO) for identification of enteric glial cells (44). Intestinal integrity was examined by staining for the tight junctional protein Zonula Occludens-1 (ZO-1; Invitrogen). For general morphological evaluation in the fetal intestine, hematoxylin and eosin (H&E) staining was performed.

As secondary antibodies, Texas Red–conjugated goat anti-rabbit from Southern Biotechnology; biotin-conjugated swine anti-rabbit or goat anti-mouse from DAKO; cytomation and peroxidase-conjugated goat anti-rabbit from Jackson ImmunoResearch Laboratories or goat anti-mouse from DAKO were used.

Immunohistochemistry

Formalin-fixed terminal ileum was embedded in paraffin, and 4- μ m sections were cut. After deparaffinization and rehydration, endogenous peroxidase activity was blocked with either 0.3% H_2O_2 diluted in Tris-buffered saline (TBS; MPO), PBS (CD3, NeuN, 5-HT, synaptophysin) or methanol (SMA22, Ki67). Nonspecific binding was blocked with normal goat serum (MPO, Ki67, NeuN, synaptophysin) or bovine serum albumin (CD3, SMA22, 5-HT) for 30 min at room temperature. Thereafter, sections were incubated with the primary antibody of interest and subsequently incubated with the selected secondary conjugated antibody. CD3, Ki67, synaptophysin, SMA22 and 5-HT antibodies were recognized with the streptavidin-biotin method (DakoCytomation), and antibodies against MPO and NeuN were detected using a peroxidase-conjugated secondary antibody. Substrate staining for MPO and SMA22 was performed with 3-amino-9-ethylcarbazole (AEC, Sigma); hematoxylin (MPO and SMA22) and nuclear fast red (CD3, Ki67, NeuN, synaptophysin and 5-HT) were used as counterstain for nuclei, respectively. Immunoreactivity for CD3, Ki67, NeuN, synaptophysin and 5-HT was detected using nickel-DAB.

Quantification of Immunohistochemical Stainings

Pictures were taken with a light microscope (Leica Microsystems CTG, type DFC295) using Leica QWin Pro version 3.4.0 software (Leica Microsystems) or with the Olympus Research System Microscope AX70 Brightfield (Olympus Corporation) using the CellProfiler software (Broad Institute), as appropriate. The positive-stained cells were counted in five high-power fields. The average number of positive cells per high-power field per animal is given. Quantification was performed as previously described (45). In brief, the high-power field was defined using the microscope, a picture was taken, and the cells were counted

immediately after on the computer screen using ImageJ. To verify accurate cell counting, the high-power field was still defined under the microscope during counting on the computer screen. The next high-power field was defined only after finishing the counting per picture. For the CD3 and MPO quantification, the total number of CD3⁺ cells was counted in the mucosa, and the MPO⁺ cells were also counted in the upper two-thirds of the villi. The thickness of the muscle layers was measured using a marker for SMA. The proliferation rate (%) in the muscle layers was determined by counting the Ki67⁺ and Ki67⁻ cells in a determined area, and the percentage of Ki67⁺ cells/total cells was calculated and expressed per 1000 μm^2 . The number of nuclei and the hypertrophy index in the muscles were calculated as previously described (46). Briefly, the total number of nuclei in muscles was calculated by counting the number of nuclei in muscle layers in a determined area, then multiplying by the surface area (μm^2) occupied by each muscle layer per power field, and the mean total cell count is presented. The hypertrophy index was calculated by dividing the total number of nuclei by the muscle surface (μm^2) and is expressed per 1000 μm^2 . The number of neuronal nuclei (NeuN⁺ cells) was counted in the ganglia of myenteric plexus. In addition, the area fractions (%) of synaptophysin and 5-HT (serotonin) were determined in ganglia of myenteric plexus (47). 5-HT⁺ cells were also counted in the mucosa, as 5-HT is expressed by enterochromaffin cells (48). Stainings were evaluated by three independent observers, who were blinded to the experimental groups.

Immunofluorescence

Fetal ileum embedded in optimal cutting temperature solution was cut at a thickness of 4 μm for immunofluorescence staining of GFAP and ZO-1 as previously reported (49). After fixation (15 min in 4% paraformaldehyde), the sections were incubated with 5% normal goat serum in 1% Tween-20 (GFAP) or 10% normal goat serum (ZO-1) for

15 min to block the nonspecific binding, and thereafter, sections were incubated overnight with GFAP or ZO-1 as a primary antibody. The next day, sections were washed and then incubated with Texas Red-conjugated secondary antibody. After 1 h of incubation, nuclei were stained with 4',6'-diamino-2-phenyl indole (DAPI) for 2 min. Finally, sections were mounted with fluorescent mounting solution. The immunoreactivity of GFAP was evaluated using a Leica DMI 4000 inverted fluorescence microscope using LAS AF software. The ZO-1 stained tight junctions were evaluated using an AxioCam MRc5 camera (Zeiss) mounted on an ECLIPSE E800 fluorescence microscope (Nikon).

RNA Isolation and Quantitative Real-Time Polymerase Chain Reaction

The messenger RNA (mRNA) levels of cytokines were measured by quantitative real-time polymerase chain reaction (qPCR) as previously described (45). RNA was extracted from ileum by the Trizol/chloroform method. Reverse transcription was achieved using M-MLV reverse transcriptase (Invitrogen) according to the supplier's guidelines. The qPCR reaction was performed with the LightCycler 480 SensiMix SYBR master mix (GC Biotech BV) in a LightCycler 480 with specific ovine primers (Supplementary Table S1). The results were normalized to the housekeeping gene ovine 40S ribosomal protein S15 (*ovRPS15*), and mean fold changes relative to control levels are presented.

Statistical Analysis

Data are presented as mean \pm standard error of the mean. Statistical analysis was performed using GraphPad Prism software (version 5.0; GraphPad Software) using a nonparametric Kruskal-Wallis test followed by Dunn's *post hoc* test. Nonparametric analysis was used based on two criteria: (1) low number of animals per group and (2) visual inspection of data in histograms, which indicated that our results did not follow a Gaussian distribution. Only differences that were

considered statistically significant at $p < 0.05$ are indicated in the figures.

All supplementary materials are available online at www.molmed.org.

RESULTS

Fetal HI Induced Intestinal Inflammation

We assessed the inflammatory response in the fetal gut 7 d after UCO by immunohistochemical staining for CD3 and MPO, which are markers for T lymphocytes and neutrophils, respectively. Total numbers of MPO⁺ cells in the intestinal mucosa did not differ between the groups (data not shown). However, fetal HI resulted in increased numbers of MPO⁺ cells in the upper part of the intestinal villi 7 d after UCO compared with control animals (Figure 2). Similarly, when animals were treated with MSCs after UCO, elevated numbers of MPO⁺ cells were found in the villus tips compared with control and MSC-treated animals (Figure 2C).

The number of CD3⁺ cells in the intestinal mucosa remained unaltered in all experimental groups compared with control animals 7 d after UCO (Figure 3C). However, fetal HI resulted in significant CD3⁺ cell influx in the circular muscle 7 d after UCO compared with control, and was not prevented by MSC treatment (Figures 3A, B and D). Importantly, the significant increase of CD3⁺ cells in the circular muscle of the HI + MSC group was maintained, even in the absence of the highest value within this HI + MSC group (Figure 3D).

We further characterize the intestinal inflammatory response by measuring mRNA levels of interleukin (*IL*)-1 β and *IL*-17, two proinflammatory cytokines with mitogenic capacities that are upregulated following HI (12,50). Fetal HI, with or without MSC treatment, increased the intestinal mRNA levels of *IL*-1 β compared with control (Figure 4A). Similarly, increased mRNA levels of *IL*-17 were detected in the fetal gut after HI compared with control. No significant changes

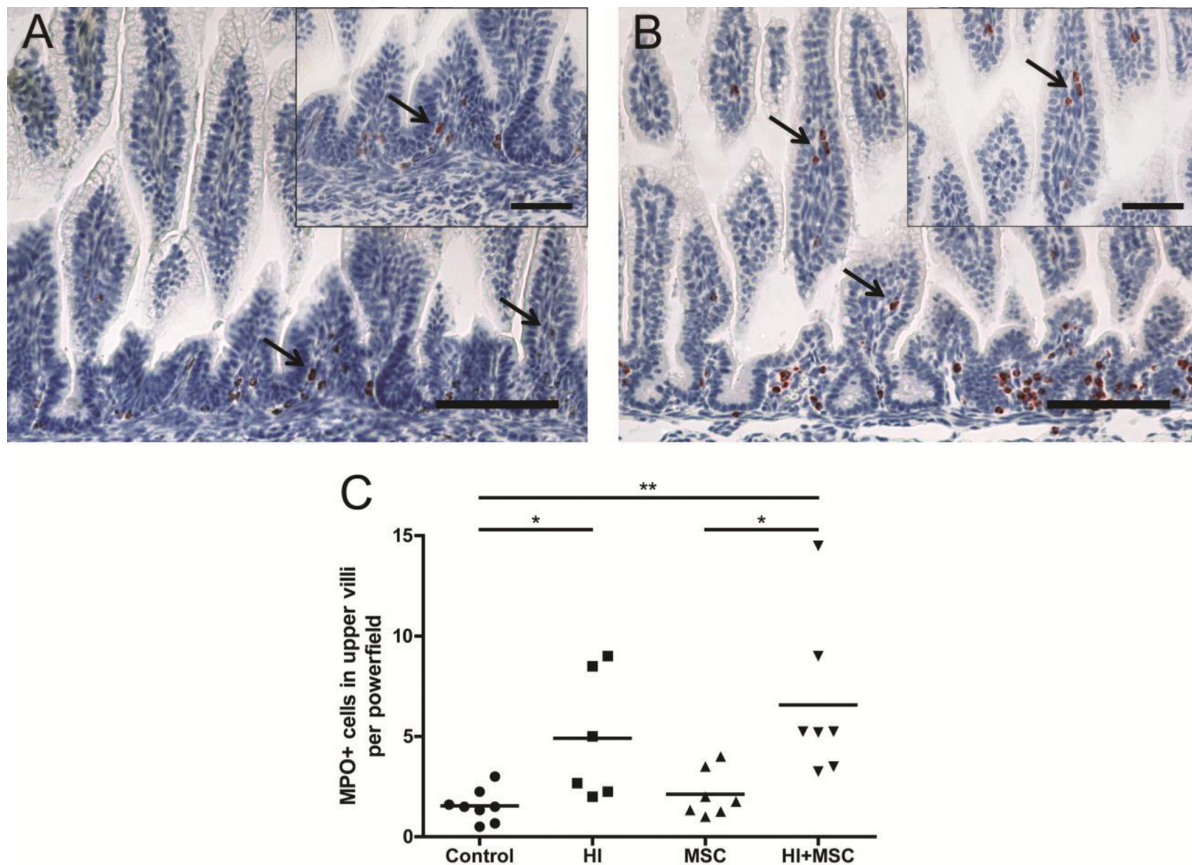


Figure 2. Increased number of MPO⁺ cells in the upper part of the villi 7 d after HI. Representative intestinal sections of (A) control and (B) HI animals were stained by immunohistochemistry for MPO. For each experimental group, MPO⁺ cells (arrows) in the upper part of the villi were counted, and the mean cell counts per power field per animal are given (C). The scale bar in panels A and B represents 100 μ m. The scale bar in insets represents 50 μ m. * p < 0.05, ** p < 0.01.

were found in *IL-17* mRNA levels of the remaining groups (Figure 4B).

Morphological Changes of the Fetal Intestine After Global HI

We performed H&E staining to assess morphological changes in the fetal ileum 7 d after fetal HI. No clear signs of epithelial injury were seen between the experimental groups (Supplementary Figure S1). Consistently, with the exception of one HI animal, no signs of tight junctional loss were found, as evaluated by immunofluorescence staining of ZO-1 (data not shown). In addition, H&E staining revealed variation in the thickness of both the circular and the longitudinal muscle layers between the groups (Supplementary Figure S1).

Fetal HI Induced Intestinal Muscle Thickness

Because the H&E staining revealed variation in the muscle layers between the experimental groups, we evaluated the effects of fetal HI in the circular and longitudinal muscle layer by immunohistochemical staining for SMA22, a marker for SMA (51). Seven days after UCO, increased muscle thickness was observed in circular and longitudinal muscle layers compared with control animals (Figures 5A–D). This increased thickness was not prevented in animals that were treated with MSCs after UCO compared with control (Figures 5C, D).

To evaluate whether the increased thickening of the muscle layers was associated with increased cell proliferation,

we stained the circular and longitudinal muscle layers for Ki67 as a marker for proliferation. Compared with control animals, the proliferation rate in the circular and longitudinal muscle layers was increased 7 d after UCO (Figures 6A–D). This increased proliferation rate of cells in the circular and longitudinal muscle layers of animals subjected to HI was not affected by MSC treatment (Figures 6C, D).

To determine whether hyperplasia (increased cell numbers) or hypertrophy (increased cell size) was responsible for the increased thickness of the circular and longitudinal muscle layers, we assessed the number of cells within the muscle layers. Fetal HI, with or without MSC treatment, increased the numbers of cells in both the longitudinal

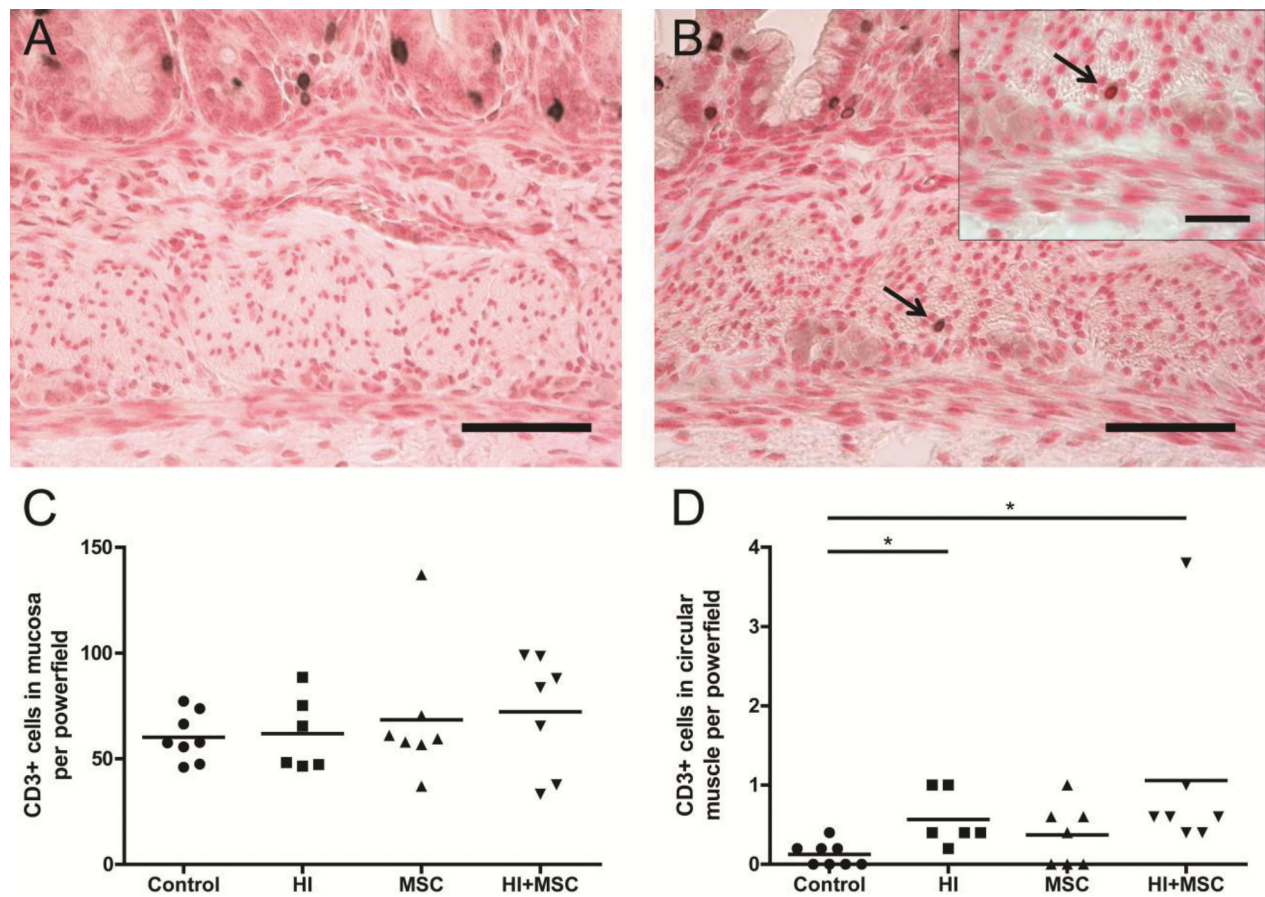


Figure 3. Invasion of CD3⁺ cells in the circular muscle layer 7 d after HI. Representative intestinal sections of (A) control and (B) HI animals were stained by immunohistochemistry for CD3. For each experimental group, CD3⁺ cells (arrow) in the mucosa (C) and circular muscle layer (D) were counted, and the mean cell counts per power field per animal are given. The scale bar in panels A and B represents 50 μ m. The scale bar in insets represents 20 μ m. * $p < 0.05$.

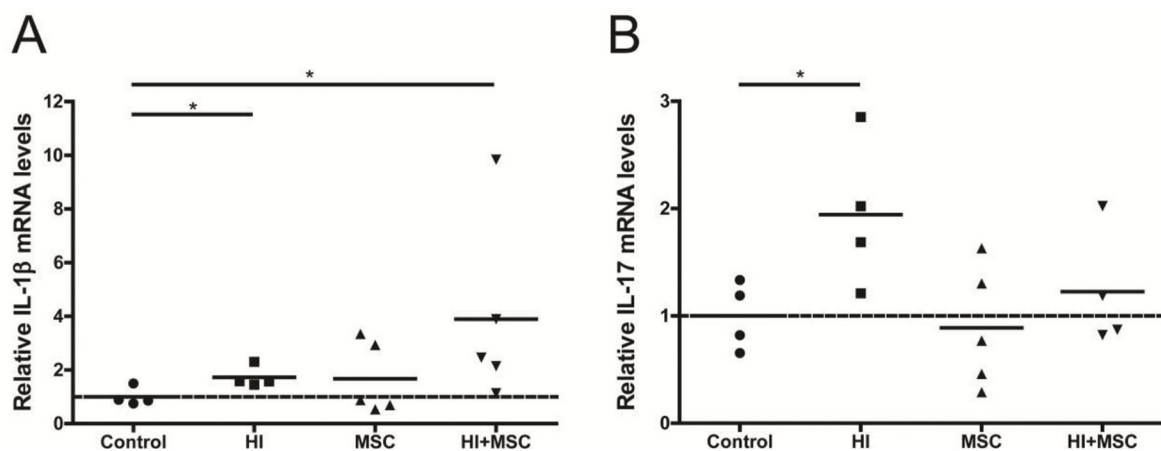


Figure 4. Increased mRNA levels of inflammatory cytokines in the fetal intestinal tissue 7 d after global HI. The inflammatory cytokines (A) IL-1 β and (B) IL-17 were assessed by quantitative real-time PCR. * $p < 0.05$.

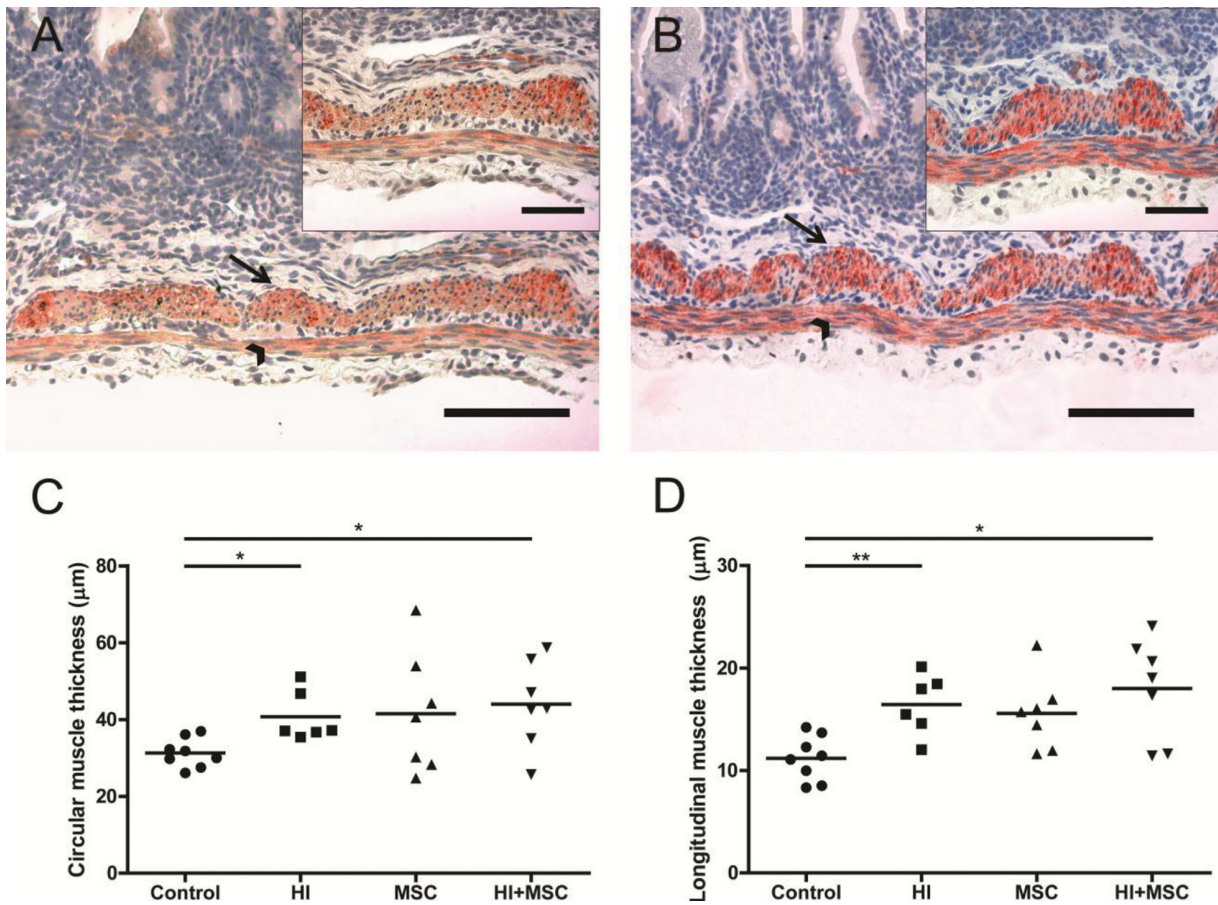


Figure 5. Increased thickness of the longitudinal and circular muscle layers 7 d after HI. Representative intestinal sections of (A) control and (B) HI animals were stained by immunohistochemistry for SMA22 (red). For each experimental group, muscle thickness in (C) circular (arrow) and (D) longitudinal (arrowhead) muscle layers was measured and the mean thickness per power field per animal is given. The scale bar in panels A and B represents 100 μm. The scale bar in insets represents 50 μm. * $p < 0.05$, ** $p < 0.01$.

and circular muscle layers compared with controls (Figures 6E, F). In contrast, no differences were found in the hypertrophy index between the groups in both muscle layers (data not shown).

Fetal HI Induced Changes in the Fetal ENS

We investigated the impact of global HI in the ganglia of myenteric plexus, which are involved in the regulation of intestinal motility (52). We first counted the number of NeuN⁺ cells (neurons) in the myenteric plexus by immunohistochemistry. The number of NeuN⁺ cells in the myenteric ganglia remained at baseline levels in all investigated groups (Figures 7A–C). We then examined

whether fetal HI induced structural changes in the enteric glial cells by immunofluorescent staining for glial fibrillary acidic protein (GFAP). The myenteric ganglia of control animals appeared with normal GFAP immunoreactivity where the perinuclear rim and glial processes were evident (Figure 8A). In contrast, animals that were subjected to UCO showed distorted GFAP immunoreactivity where glial processes were absent and GFAP globules were displayed (Figure 8B). The distortion of GFAP immunoreactivity following fetal HI was not prevented by MSC treatment (data not shown).

We evaluated whether fetal HI induced changes in intestinal neuronal

synapses and signaling by staining for synaptophysin and 5-HT (serotonin), respectively. Global HI induced an increased positive-stained area of synaptophysin in the ganglia of myenteric plexus compared with control animals (Figure 9), whereas no changes were found in the expression of synaptophysin in the remaining groups compared with control (Figure 9C). The positive-stained area of 5-HT in myenteric ganglia was increased 7 d after fetal HI (Figure 10D). Similarly, increased expression of 5-HT was found when animals were treated with MSCs after UCO compared with control (Figure 10D). In addition, fetal HI increased the numbers of 5-HT⁺ cells in the mucosa (Figures 10A–C), whereas

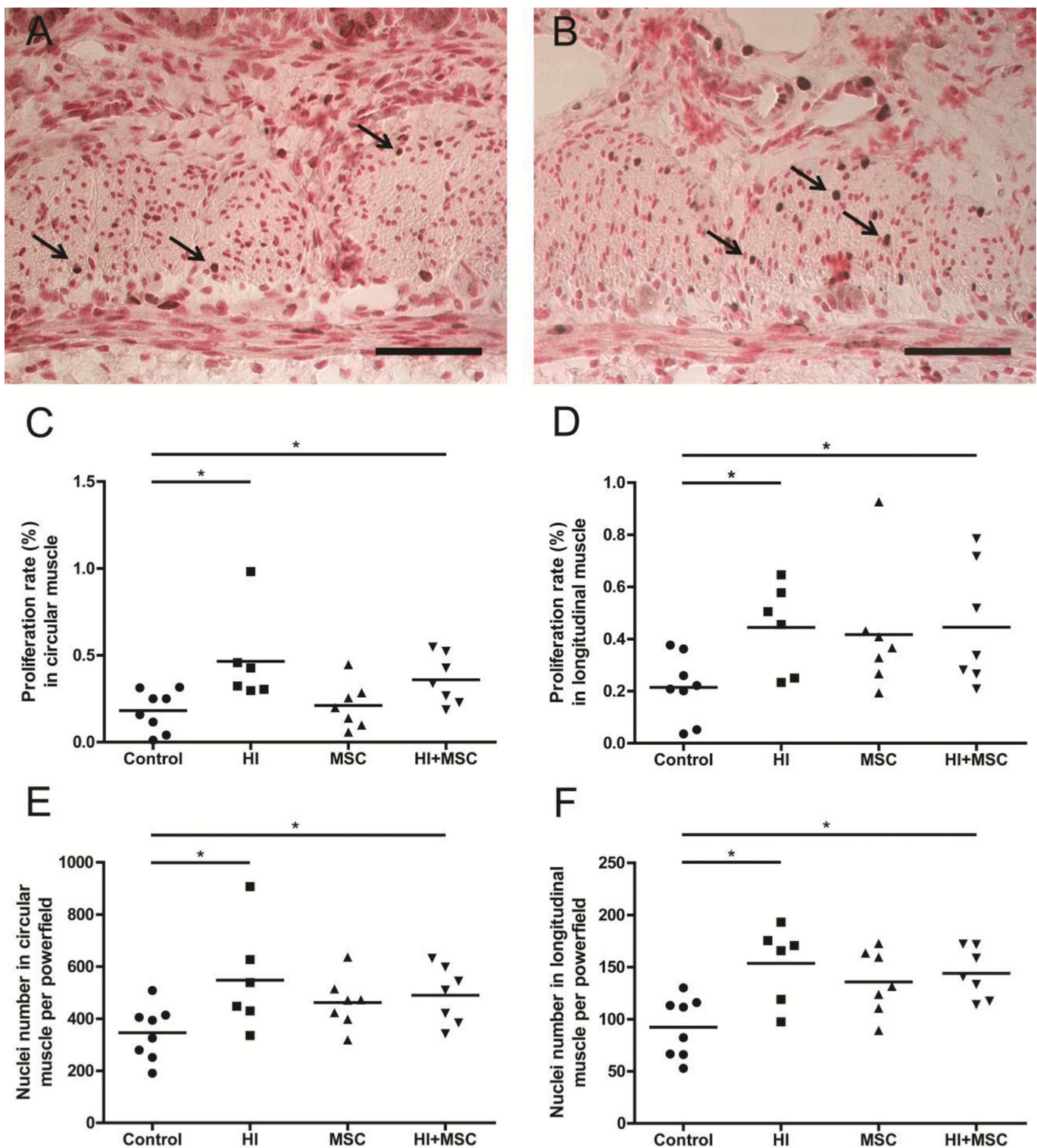


Figure 6. Increased proliferation rate and number of nuclei in muscle layers 7 d after HI. Representative intestinal sections of (A) control and (B) HI animals were stained by immunohistochemistry for Ki67. For each experimental group, proliferation rate in (C) circular and (D) longitudinal and nuclei numbers in (E) circular and (F) longitudinal muscle layer were counted, and the mean cell counts per power field per animal are given. The proliferation rate (%) is expressed per 1000 μm^2 . The arrows indicate Ki67⁺ cells within the muscle layers. The scale bar in panels A and B represents 50 μm . * $p < 0.05$.

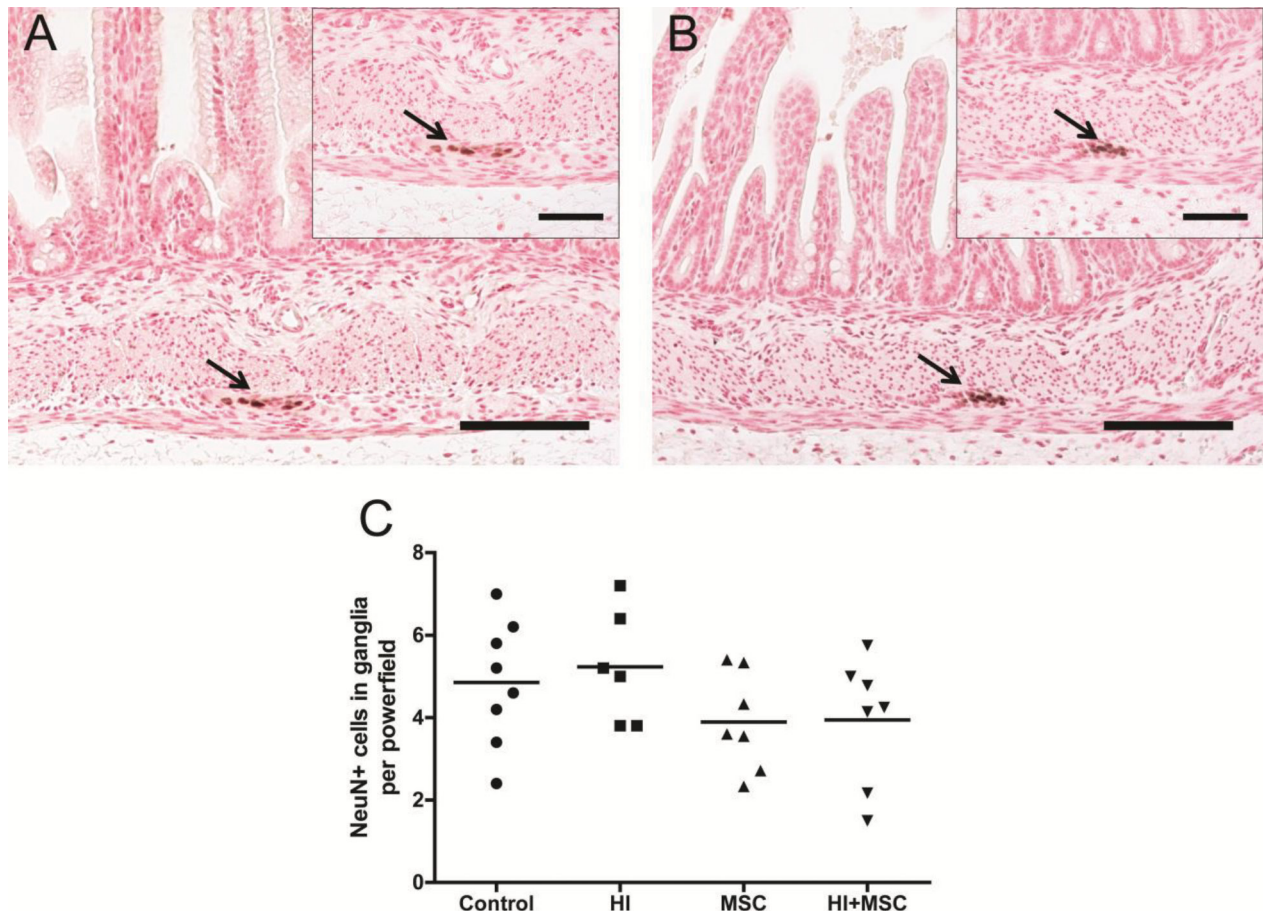


Figure 7. Number of NeuN⁺ cells in myenteric plexus 7 d after HI. Representative gut sections of (A) control and (B) HI animals were stained by NeuN, a marker for neuronal nuclei. The number of NeuN⁺ cells (arrows) in myenteric ganglia remained at baseline level (C). The scale bar in panels A and B represents 100 μ m. The scale bar in insets represents 50 μ m.

no changes were detected in animals that were treated with MSCs, with or without UCO, compared with control (Figure 10C).

DISCUSSION

In this study, we used a preclinical ovine model to investigate the impact of fetal HI on the preterm gut and to assess the potential of intravenous administration of MSCs to improve the outcome of the postischemic intestine. Our data demonstrated that fetal global HI caused intestinal inflammation accompanied by thickening of the muscle layers, distortion of enteric glial cells and altered expression of mediators involved in neurotransmission in the preterm gut. These adverse intestinal outcomes induced by

global HI were not attenuated by intravenous administration of MSCs.

Intestinal inflammation following fetal HI in our model was characterized by accumulation of neutrophils in the villus tips. Infiltration of neutrophils in the mucosa, as seen in the preterm fetal gut following global HI, has also been detected in adult rodent models of intestinal HI induced by transient superior mesenteric artery occlusion (13,14,53). Interestingly, in this study, the influx of neutrophils was not associated with epithelial injury in villus tips, the first mucosal structures that are affected following intestinal HI (17,54). This could be explained by the fact that damage to the enterocytes following intestinal HI in human and

animal studies occurs acutely after the insult with sealing of the epithelial lining and re-epithelialization being documented within a few hours to a couple of days after the end of local intestinal HI (54–56). Our findings suggest that in the absence of epithelial injury, which most likely was resolved 7 d after UCO, inflammatory processes in the intestinal mucosa persisted and might be responsible for some of the adverse intestinal effects in the lower layers of the gastrointestinal wall (57) as discussed below.

Intestinal immune activation below the submucosa was characterized by invasion of T lymphocytes into the circular muscle layer following fetal HI, which is consistent with previous findings (56,58). The invasion of T cells into the circular

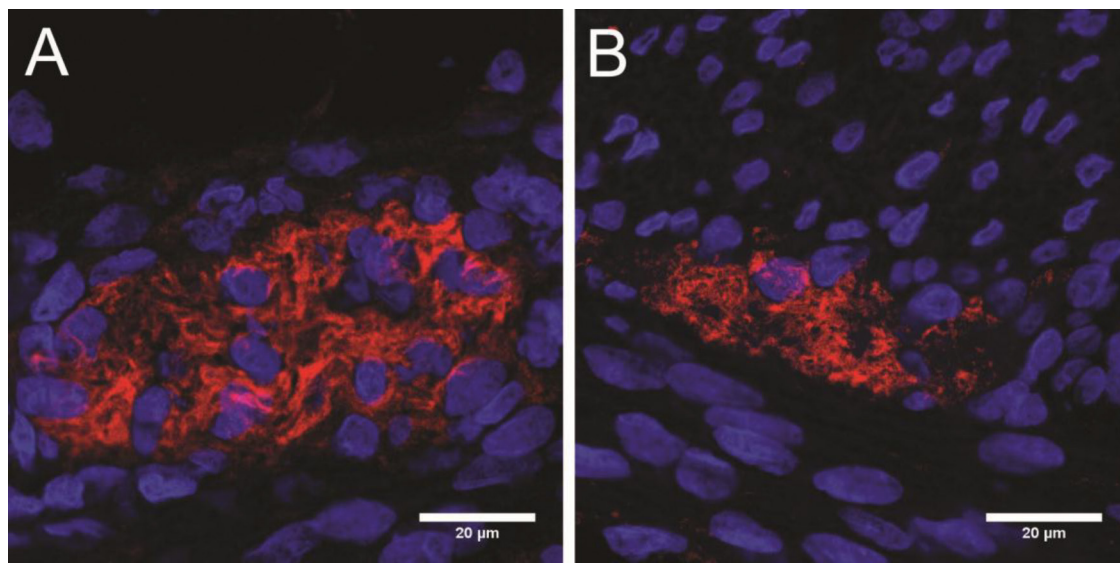


Figure 8. Distortion of enteric glial cells in myenteric plexus 7 d after HI. Representative sections of fetal ileum stained by immunofluorescence for GFAP (red), a marker for enteric glial cells, and DAPI (blue), a marker for nuclei. Control animals appeared with normal perinuclear GFAP immunoreactivity and intact glial processes (A), whereas animals subjected to HI appeared with loss of GFAP immunoreactivity around the nuclei and aggregates of GFAP without clear enteric glial processes (B).

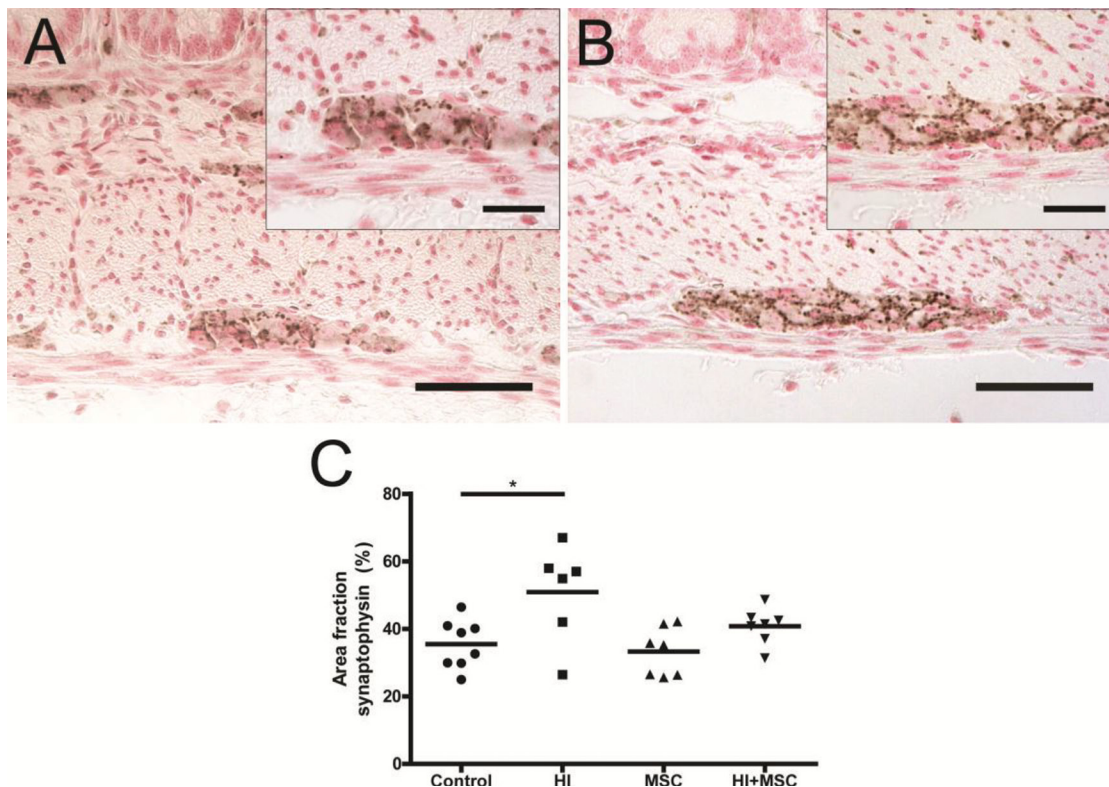


Figure 9. Increased expression of synaptophysin in myenteric ganglia 7 d after HI. Representative intestinal sections of (A) control and (B) HI animals were stained by immunohistochemistry for synaptophysin. For each experimental group, the synaptophysin-positive area in myenteric ganglia was measured and the mean area fraction (%) per ganglion per animal is given (C). The scale bar in panels A and B represents 50 µm. The scale bar in insets represents 20 µm. * $p < 0.05$.

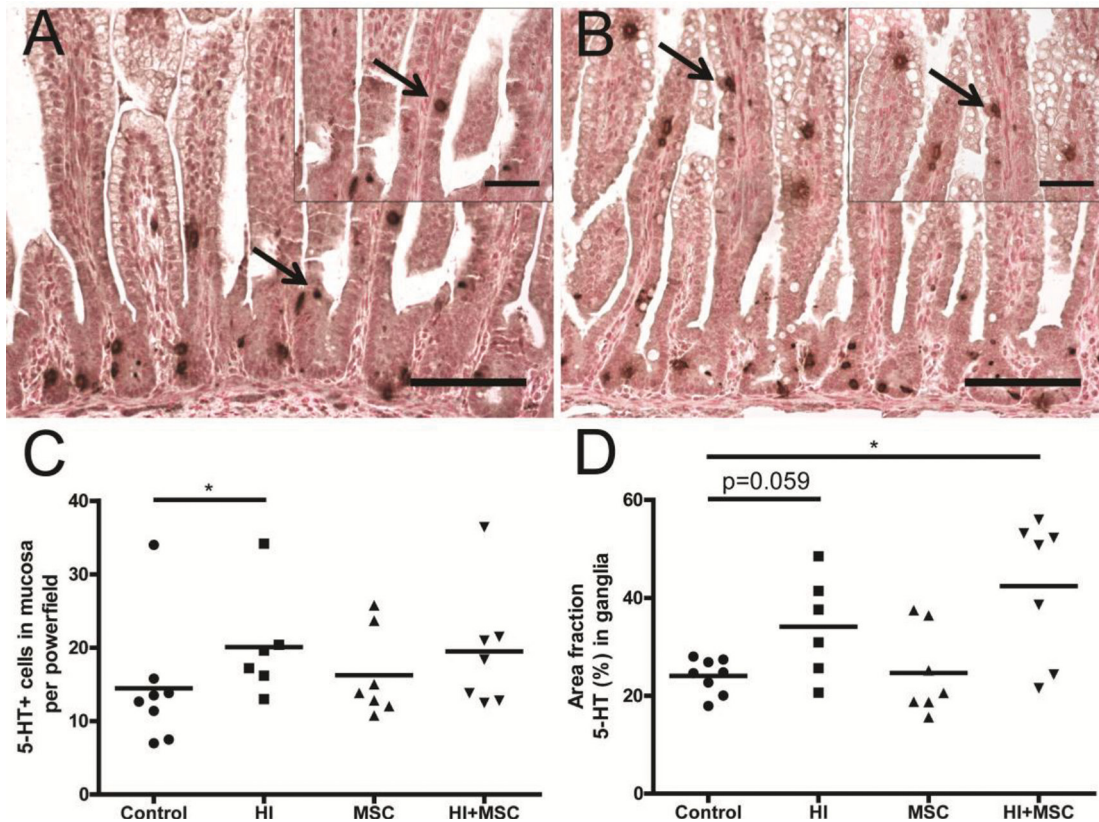


Figure 10. Increased 5-HT in fetal intestinal mucosa 7 d after HI. Representative intestinal sections of (A) control and (B) HI animals were stained by immunohistochemistry for 5-HT. For each experimental group, 5-HT⁺ cells (arrows) in mucosa (C) were counted and the 5-HT-positive area in myenteric ganglia (D) was measured. The mean cell counts in mucosa and area fraction (%) per ganglion per animal are given. The scale bar in panels represents 100 μ m. The scale bar in insets represents 50 μ m. * p < 0.05. Significance between control and HI group in panel D was tested by t test, and p value is given.

muscle (but not into longitudinal) 7 d after fetal HI could be explained by the different anatomical positions of the two muscle layers within the intestinal wall. The circular muscle layer is closer to the mucosa/submucosa layer, where an inflammatory response is initiated by resident immune cells upon a stressor stimulus (59). Moreover, previous studies have shown that adhesion of T lymphocytes was preferentially found in the submucosa and not in muscle venules of the postischemic intestine (60,61). Therefore, the influx of T lymphocytes in the muscularis of the postischemic intestinal wall in our model is more likely to occur first in the circular muscle layer.

Intestinal inflammation in the mucosa and muscle layers following fetal HI was associated with thickening of the smooth

muscle, which has been previously described in rodent models of transient superior mesenteric artery occlusion (58). The inflammation-induced thickening of the circular and longitudinal muscle layers could be explained by several mechanisms, including hypertrophy and/or secretion of inflammatory cytokines, which are considered to have mitogenic effects on muscle cells (46,50,62). In line with these reports, muscle thickening after HI in our animal model was accompanied by increased cell numbers and cell proliferation within the muscle layers of the fetal intestine and elevated mRNA levels of *IL-1 β* and *IL-17*, two proinflammatory cytokines that are known to promote intestinal muscle growth (50). Therefore, we speculate that the inflammatory cytokines *IL-1 β* and

IL-17 may contribute to the muscle hyperplasia detected 7 d after UCO. Importantly, muscle thickening characterizes the inflamed gut of several gastrointestinal diseases and has been correlated with altered intestinal smooth muscle contractility (57,63).

In addition to smooth muscle contractions, the ENS is essential for coordinated gastrointestinal motility (52,64). In this regard, enteric glial cells are ideally positioned around enteric neurons to respond to and modulate neural activity by several mechanisms, including terminating the actions of neurotransmitters from synapses and generating neuroactive substances. The regulatory role of enteric glial cells in gastrointestinal function is further highlighted by experiments demonstrating

that disruption of these cells altered the neurochemical phenotype of enteric neurons, reduced transmission to muscle and delayed gastrointestinal transit (65,66). In this study, global HI-induced distortion of enteric glial cells in the ganglia of the myenteric plexus in a similar pattern found in animal models of HI-induced intestinal injury (67) and in neonates with NEC (31). Importantly, distortion of enteric glial cells upon gut HI has been correlated with loss of enteric neurons and impaired neuronal function, with subsequent decreased gastrointestinal motility (18,44,67,68). Gastrointestinal dysfunction might lead to vomiting, with subsequent delay in tolerating enteral feeding postnatally, resulting in intestinal immaturity, as early initiation of enteral nutrition is crucial for normal gut development (69). Although the number of enteric neurons remained unaltered following fetal HI in our model, overexpression of synaptophysin, a crucial regulator of neurotransmission (70), was detected in the ganglia of myenteric plexus of the fetal postischemic gut, implying enhanced probability of neurotransmitter release (71) and/or abnormal intestinal motor function (72,73). This finding is supported by the increased expression of serotonin, a neurotransmitter that regulates intestinal motility, in the myenteric ganglia following HI, and its disrupted homeostasis has been correlated with several gastrointestinal inflammatory and motility disorders (74). In addition to the elevated expression of neuronal serotonin, global HI increased the number of serotonin-positive cells along the intestinal mucosa. Such alterations in the mucosal-derived serotonin contribute to intestinal dysmotility (48) and have been associated with inflammatory bowel disease (75). Importantly, NEC has been associated with maternal use of selective serotonin reuptake inhibitors during pregnancy (76).

In this study, intravenous administration of MSCs did not ameliorate the adverse effects of fetal global HI on the preterm gut, whereas this treatment was previously shown to protect the fetal

brain from structural and functional impairment associated with T-cell tolerance (32). Although MSCs have been proven beneficial when given intramuscularly (77–79) or intraperitoneally (80) in animal models of intestinal HI, in this study we deliberately chose to administer the MSCs intravenously, since it was previously shown that this yielded better engraftment of MSCs to the fetal gut compared with intraperitoneal administration (23), and this could have beneficial effects not only in the gut but in multiple organs that are affected by global HI. In addition, the relative impact of global HI on the fetal gut is essentially lower compared with other vital organs, such as HI-induced cerebral injury. Because MSCs have the tendency to migrate toward inflammatory tissues (81), it is conceivable that intravenous administration of MSCs following global HI would primarily lead to engraftment of these stem cells in the inflamed organs that are most severely affected. Accordingly, we previously showed that 7 d after intravenous administration, low numbers of MSCs were present in the fetal spleen and lung and occasionally in the brain (but not in the gut), accompanied by prevention of brain injury in our model (32). Therefore, the preferential distribution of MSCs following global HI might explain the lack of therapeutic effects on the fetal gut. Although the dosage of MSCs that was used in this study was based on clinical trials of focal ischemia (28) and patients with inflammatory bowel disease (29,30), it is conceivable that higher numbers of MSCs with repeated doses at subsequent time points might increase the chance for MSC engraftment into the gut and potentially improve the intestinal outcome following global HI.

CONCLUSION

The preterm hypoxic-ischemic fetus and infant are especially vulnerable to functional gastrointestinal impairment during the first days of life. The clinical pathological intestinal characteristics of an hypoxic-ischemic neonate may

include delayed gastrointestinal transit, which frequently precedes abdominal distension, inflammation, and edema of the intestine (82,83). These factors predispose the preterm hypoxic-ischemic gut not only to feeding intolerance, but also to NEC. In this study, we showed that global HI in fetal sheep induced intestinal inflammation, muscle thickening, distortion of enteric glial cells and altered neurotransmission. Although we can only speculate about the postnatal consequences of these adverse intestinal outcomes, the detected gut inflammation and ENS abnormalities following HI have been associated with neonatal gastrointestinal complications including loss of barrier integrity, delayed gastrointestinal motility and NEC (31,73,84). Future studies are warranted to investigate whether the detected pathological changes 7 d after UCO will have long-term adverse intestinal effects. In addition, MSC treatment did not protect the fetal gut against HI-induced intestinal abnormalities, but it did prevent HI-induced cerebral injury. Because our data suggest selective organ protection after intravenous MSC treatment, future studies should focus on optimizing an MSC-based treatment regimen that will collectively protect the fetal brain and gut following global HI.

DISCLOSURE

The authors declare that they have no competing interests as defined by *Molecular Medicine*, or other interests that might be perceived to influence the results and discussion reported in this paper.

REFERENCES

1. Alonso-Spilsbury M, et al. (2005) Perinatal asphyxia pathophysiology in pig and human: A review. *Anim. Reprod. Sci.* 90:1–30.
2. Tax N, et al. (2013) The influence of perinatal asphyxia on peripheral oxygenation and perfusion in neonates. *Early Hum. Dev.* 89:483–486.
3. Daripa M, et al. (2013) Perinatal asphyxia associated with early neonatal mortality: Population study of avoidable deaths. *Rev. Paul. Pediatr.* 31:37–45.
4. Lawn JE, Kerber K, Enweronu-Laryea C, Cousens S. (2010) 3.6 million neonatal deaths—what is progressing and what is not? *Semin. Perinatol.* 34:371–386.

5. Hankins GD, et al. (2002) Neonatal organ system injury in acute birth asphyxia sufficient to result in neonatal encephalopathy. *Obstet. Gynecol.* 99:688–691.
6. Shah P, Riphagen S, Beyene J, Perlman M. (2004) Multiorgan dysfunction in infants with post-asphyxial hypoxic-ischaemic encephalopathy. *Arch. Dis. Child. Fetal Neonatal Ed.* 89:F152–F155.
7. Berseth CL, McCoy HH. (1992) Birth asphyxia alters neonatal intestinal motility in term neonates. *Pediatrics.* 90:669–673.
8. Fox TP, Godavitarne C. (2012) What really causes necrotising enterocolitis? *ISRN Gastroenterol.* 2012:628317.
9. Neu J, Walker WA. (2011) Necrotizing enterocolitis. *N. Engl. J. Med.* 364:255–264.
10. Taylor CT, Cummins EP. (2009) The role of NF-kappaB in hypoxia-induced gene expression. *Ann. N. Y. Acad. Sci.* 1177:178–184.
11. Eltzschig HK, Eckle T. (2011) Ischemia and reperfusion—from mechanism to translation. *Nat. Med.* 17:1391–1401.
12. Grenz A, Clambey E, Eltzschig HK. (2012) Hypoxia signaling during intestinal ischemia and inflammation. *Curr. Opin. Crit. Care.* 18:178–185.
13. Ozban M, et al. (2015) The effect of melatonin on bacterial translocation following ischemia/reperfusion injury in a rat model of superior mesenteric artery occlusion. *BMC Surg.* 15:18.
14. Stefanutti G, Pierro A, Parkinson EJ, Smith VV, Eaton S. (2008) Moderate hypothermia as a rescue therapy against intestinal ischemia and reperfusion injury in the rat. *Crit. Care Med.* 36:1564–1572.
15. Kannan KB, et al. (2011) Hypoxia-inducible factor plays a gut-injurious role in intestinal ischemia reperfusion injury. *Am. J. Physiol. Gastrointest. Liver Physiol.* 300:G853–861.
16. Pontell L, et al. (2011) Damaging effects of ischemia/reperfusion on intestinal muscle. *Cell Tissue Res.* 343:411–419.
17. Gonzalez LM, Moeser AJ, Blikslager AT. (2015) Animal models of ischemia-reperfusion-induced intestinal injury: Progress and promise for translational research. *Am. J. Physiol. Gastrointest Liver Physiol.* 308:G63–G75.
18. Mendes CE, et al. (2015) The effect of ischemia and reperfusion on enteric glial cells and contractile activity in the ileum. *Dig. Dis. Sci.* 60:2677–2689.
19. Silva MA, de Meirelles LR, Bustorff-Silva JM. (2007) Changes in intestinal motility and in the myenteric plexus in a rat model of intestinal ischemia-reperfusion. *J. Pediatr. Surg.* 42:1062–1065.
20. Griffin MD, et al. (2013) Concise review: Adult mesenchymal stromal cell therapy for inflammatory diseases: How well are we joining the dots? *Stem Cells.* 31:2033–2041.
21. Martinez-Montiel MdP, Gomez-Gomez GJ, Flores AI. (2014) Therapy with stem cells in inflammatory bowel disease. *World J. Gastroenterol.* 20:1211–1227.
22. Nagaishi K, Arimura Y, Fujimiya M. (2015) Stem cell therapy for inflammatory bowel disease. *J. Gastroenterol.* 50:280–286.
23. Yang J, et al. (2012) Heparin-binding epidermal growth factor-like growth factor and mesenchymal stem cells act synergistically to prevent experimental necrotizing enterocolitis. *J. Am. Coll. Surg.* 215:534–545.
24. Jellema RK, et al. (2013) Cerebral inflammation and mobilization of the peripheral immune system following global hypoxia-ischemia in preterm sheep. *J. Neuroinflammation.* 10:13.
25. Uccelli A, Moretta L, Pistoia V. (2008) Mesenchymal stem cells in health and disease. *Nat. Rev. Immunol.* 8:726–736.
26. Ma S, et al. (2014) Immunobiology of mesenchymal stem cells. *Cell Death Differ.* 21:216–225.
27. Parekkadan B, Milwid JM. (2010) Mesenchymal stem cells as therapeutics. *Annu. Rev. Biomed. Eng.* 12:87–117.
28. Bang OY, Lee JS, Lee PH, Lee G. (2005) Autologous mesenchymal stem cell transplantation in stroke patients. *Ann. Neurol.* 57:874–882.
29. Duijvestein M, et al. (2010) Autologous bone marrow-derived mesenchymal stromal cell treatment for refractory luminal Crohn's disease: Results of a phase I study. *Gut.* 59:1662–1669.
30. Dalal J, Gandy K, Domen J. (2012) Role of mesenchymal stem cell therapy in Crohn's disease. *Pediatr. Res.* 71:445–451.
31. Zhou Y, et al. (2013) Enteric nervous system abnormalities are present in human necrotizing enterocolitis: Potential neurotransplantation therapy. *Stem Cell Res. Ther.* 4:157.
32. Jellema RK, et al. (2013) Mesenchymal stem cells induce T-cell tolerance and protect the preterm brain after global hypoxia-ischemia. *PLoS One.* 8:e73031.
33. Back SA, Riddle A, Dean J, Hohimer AR. (2012) The instrumented fetal sheep as a model of cerebral white matter injury in the premature infant. *Neurotherapeutics.* 9:359–370.
34. Roelfsema V, et al. (2004) Window of opportunity of cerebral hypothermia for postischemic white matter injury in the near-term fetal sheep. *J. Cereb. Blood Flow Metab.* 24:877–886.
35. Jellema RK, et al. (2013) Systemic G-CSF attenuates cerebral inflammation and hypomyelination but does not reduce seizure burden in preterm sheep exposed to global hypoxia-ischemia. *Exp. Neurol.* 250:293–303.
36. Bennet L, et al. (2007) The effect of cerebral hypothermia on white and grey matter injury induced by severe hypoxia in preterm fetal sheep. *J. Physiol.* 578:491–506.
37. Wassink G, et al. (2007) The ontogeny of hemodynamic responses to prolonged umbilical cord occlusion in fetal sheep. *J. Appl. Physiol.* (1985). 103:1311–1317.
38. Bennet L, Quaedackers JS, Gunn AJ, Rossenrode S, Heineman E. (2000) The effect of asphyxia on superior mesenteric artery blood flow in the preterm sheep fetus. *J. Pediatr. Surg.* 35:34–40.
39. Bennet L, et al. (2007) Regulation of cytochrome oxidase redox state during umbilical cord occlusion in preterm fetal sheep. *Am. J. Physiol. Regul. Integr. Comp. Physiol.* 292:R1569–R1576.
40. Gunn AJ, Bennet L. (2009) Fetal hypoxia insults and patterns of brain injury: Insights from animal models. *Clin. Perinatol.* 36:579–593.
41. Lear CA, et al. (2015) Subclinical decelerations during developing hypotension in preterm fetal sheep after acute on chronic lipopolysaccharide exposure. *Sci. Rep.* 5:16201.
42. Ryan M, McAdams DJL. (2015) Focal intestinal perforation in late preterm and term neonates with hypoxic ischemic encephalopathy. *J. Pediatr. Surg. Case Rep.* 3:137–139.
43. Sharma R, Hudak ML. (2013) A clinical perspective of necrotizing enterocolitis: Past, present, and future. *Clin. Perinatol.* 40:27–51.
44. Gulbransen BD, Sharkey KA. (2012) Novel functional roles for enteric glia in the gastrointestinal tract. *Nat. Rev. Gastroenterol. Hepatol.* 9:625–632.
45. Nikiforou M, et al. (2015) Prophylactic interleukin-2 treatment prevents fetal gut inflammation and injury in an ovine model of chorioamnionitis. *Inflamm. Bowel Dis.* 21:2026–2038.
46. Blennerhassett MG, Vignjevic P, Vermillion DL, Collins SM. (1992) Inflammation causes hyperplasia and hypertrophy in smooth muscle of rat small intestine. *Am. J. Physiol.* 262:G1041–G1046.
47. Martin GR, et al. (2012) Endogenous cellular prion protein regulates contractility of the mouse ileum. *Neurogastroenterol. Motil.* 24:e412–e424.
48. Crowell MD, Shetzline MA, Moses PL, Mawe GM, Talley NJ. (2004) Enterochromaffin cells and 5-HT signaling in the pathophysiology of disorders of gastrointestinal function. *Curr. Opin. Investig. Drugs.* 5:55–60.
49. Nikiforou M, et al. (2016) Selective IL-1 alpha exposure to the fetal gut, lung, and chorioamnion/skin causes intestinal inflammatory and developmental changes in fetal sheep. *Lab. Invest.* 96:69–80.
50. Nair DG, Miller KG, Lourens SR, Blennerhassett MG. (2014) Inflammatory cytokines promote growth of intestinal smooth muscle cells by induced expression of PDGF-Rbeta. *J. Cell Mol. Med.* 18:444–454.
51. Knowles CH, et al. (2004) Deranged smooth muscle alpha-actin as a biomarker of intestinal pseudo-obstruction: A controlled multinational case series. *Gut.* 53:1583–1589.
52. Furness JB. (2012) The enteric nervous system and neurogastroenterology. *Nat. Rev. Gastroenterol. Hepatol.* 9:286–294.
53. Guzman-De La Garza FJ, et al. (2010) Ketamine reduces intestinal injury and inflammatory cell infiltration after ischemia/reperfusion in rats. *Surg. Today.* 40:1055–1062.
54. Grootjans J, et al. (2011) Rapid lamina propria retraction and zipper-like constriction of the epithelium preserves the epithelial lining in human small intestine exposed to ischaemia-reperfusion. *J. Pathol.* 224:411–419.

55. Derikx JP, *et al.* (2008) Rapid reversal of human intestinal ischemia-reperfusion induced damage by shedding of injured enterocytes and reepithelialisation. *PLoS One*. 3:e3428.
56. Pontell L, *et al.* (2011) Damaging effects of ischemia/reperfusion on intestinal muscle. *Cell Tissue Res*. 343:411–419.
57. Tanovic A, Fernandez E, Jimenez M. (2006) Alterations in intestinal contractility during inflammation are caused by both smooth muscle damage and specific receptor-mediated mechanisms. *Croat. Med. J.* 47:318–326.
58. Lindstrom LM, Ekblad E. (2004) Structural and neuronal changes in rat ileum after ischemia with reperfusion. *Dig. Dis. Sci.* 49:1212–1222.
59. Maynard CL, Elson CO, Hatton RD, Weaver CT. (2012) Reciprocal interactions of the intestinal microbiota and immune system. *Nature*. 489:231–241.
60. Shigematsu T, Wolf RE, Granger DN. (2002) T-lymphocytes modulate the microvascular and inflammatory responses to intestinal ischemia-reperfusion. *Microcirculation*. 9:99–109.
61. Beuk RJ, *et al.* (2000) Total warm ischemia and reperfusion impairs flow in all rat gut layers but increases leukocyte-vessel wall interactions in the submucosa only. *Ann. Surg.* 231:96–104.
62. Nair DG, Han TY, Lourensens S, Blennerhassett MG. (2011) Proliferation modulates intestinal smooth muscle phenotype in vitro and in colitis in vivo. *Am. J. Physiol. Gastrointest. Liver Physiol.* 300:C903–913.
63. Severi C, *et al.* (2014) Contribution of intestinal smooth muscle to Crohn's disease fibrogenesis. *Eur. J. Histochem.* 58:2457.
64. Burns AJ, Roberts RR, Bornstein JC, Young HM. (2009) Development of the enteric nervous system and its role in intestinal motility during fetal and early postnatal stages. *Semin. Pediatr. Surg.* 18:196–205.
65. Aube AC, *et al.* (2006) Changes in enteric neurone phenotype and intestinal functions in a transgenic mouse model of enteric glia disruption. *Gut*. 55:630–637.
66. Sharkey KA. (2015) Emerging roles for enteric glia in gastrointestinal disorders. *J. Clin. Invest.* 125:918–925.
67. Thacker M, Rivera LR, Cho HJ, Furness JB. (2011) The relationship between glial distortion and neuronal changes following intestinal ischemia and reperfusion. *Neurogastroenterol. Motil.* 23:e500–e509.
68. Bassotti G, Villanacci V, Antonelli E, Morelli A, Salerni B. (2007) Enteric glial cells: New players in gastrointestinal motility? *Lab. Invest.* 87:628–632.
69. Strodtbeck F. (2003) The role of early enteral nutrition in protecting premature infants from sepsis. *Crit. Care Nurs. Clin. North Am.* 15:79–87.
70. Kwon SE, Chapman ER. (2011) Synaptophysin regulates the kinetics of synaptic vesicle endocytosis in central neurons. *Neuron*. 70:847–854.
71. Alder J, Kanki H, Valtorta F, Greengard P, Poo MM. (1995) Overexpression of synaptophysin enhances neurotransmitter secretion at *Xenopus* neuromuscular synapses. *J. Neurosci.* 15:511–519.
72. Dzienis-Koronkiewicz E, Debek W, Chyczewski L. (2005) Use of synaptophysin immunohistochemistry in intestinal motility disorders. *Eur. J. Pediatr. Surg.* 15:392–398.
73. Geramizadeh B, Akbarzadeh E, Izadi B, Foroutan HR, Heidari T. (2013) Immunohistochemical study of enteric nervous system in hirschsprung's disease and intestinal neuronal dysplasia. *Histol. Histopathol.* 28:345–351.
74. Gershon MD. (2013) 5-Hydroxytryptamine (serotonin) in the gastrointestinal tract. *Curr. Opin. Endocrinol. Diabetes Obes.* 20:14–21.
75. Mawe GM, Hoffman JM. (2013) Serotonin signalling in the gut—functions, dysfunctions and therapeutic targets. *Nat. Rev. Gastroenterol. Hepatol.* 10:473–486.
76. Potts AL, Young KL, Carter BS, Shenai JP. (2007) Necrotizing enterocolitis associated with in utero and breast milk exposure to the selective serotonin reuptake inhibitor, escitalopram. *J. Perinatol.* 27:120–122.
77. Shen ZY, Zhang J, Song HL, Zheng WP. (2013) Bone-marrow mesenchymal stem cells reduce rat intestinal ischemia-reperfusion injury, ZO-1 downregulation and tight junction disruption via a TNF-alpha-regulated mechanism. *World J. Gastroenterol.* 19:3583–3595.
78. Jiang H, *et al.* (2013) Potential role of mesenchymal stem cells in alleviating intestinal ischemia/reperfusion impairment. *PLoS One*. 8:e74468.
79. Jiang H, *et al.* (2011) Bone marrow mesenchymal stem cells reduce intestinal ischemia/reperfusion injuries in rats. *J. Surg. Res.* 168:127–134.
80. Watkins DJ, Yang J, Matthews MA, Besner GE. (2013) Synergistic effects of HB-EGF and mesenchymal stem cells in a murine model of intestinal ischemia/reperfusion injury. *J. Pediatr. Surg.* 48:1323–1329.
81. Eggenhofer E, Luk F, Dahlke MH, Hoogduijn MJ. (2014) The life and fate of mesenchymal stem cells. *Front. Immunol.* 5:148.
82. Neu J. (2007) Gastrointestinal development and meeting the nutritional needs of premature infants. *Am. J. Clin. Nutr.* 85:629S–634S.
83. Commare CE, Tappenden KA. (2007) Development of the infant intestine: Implications for nutrition support. *Nutr. Clin. Pract.* 22:159–173.
84. Khen N, *et al.* (2004) Fetal intestinal obstruction induces alteration of enteric nervous system development in human intestinal atresia. *Pediatr. Res.* 56:975–980.

Cite this article as: Nikiforou M, *et al.* (2016) Global hypoxia-ischemia induced inflammation and structural changes in the preterm ovine gut which were not ameliorated by mesenchymal stem cell treatment. *Mol. Med.* 22:244–57.